nature research

https://doi.org/10.1038/s41558-020-00909-3

Supplementary information

Dust dominates high-altitude snow darkening and melt over high-mountain Asia

In the format provided by the authors and unedited

Supplementary Information for

Dust dominates high-altitude snow darkening and melt over high-mountain Asia

Chandan Sarangi[1,2*], Yun Qian[1*], Karl Rittger[3], L. Ruby Leung[1], Duli Chand[1], Kat J. Bormann[4], Thomas H. Painter[5]

----

[1]Pacific Northwest National Laboratory

[2]Indian Institute of Technology Madras, Chennai, Tamil Nadu, India

[3]Institute of Arctic and Alpine Research, University of Colorado, Boulder

[4]Jet Propulsion Laboratory, California Institute of Technology

[5]JIFRESSE, University of California, Los Angeles

*Correspondence to yun.qian@pnnl.gov and chandansarangi@iitm.ac.in

---

Keywords: Elevated aerosol layers (EAL), Light absorbing particles (LAP), snow albedo darkening, Indus basin, Dust, High Mountain Asia (HMA)

This document contains supplementary Figures

Figures: S1 to S11

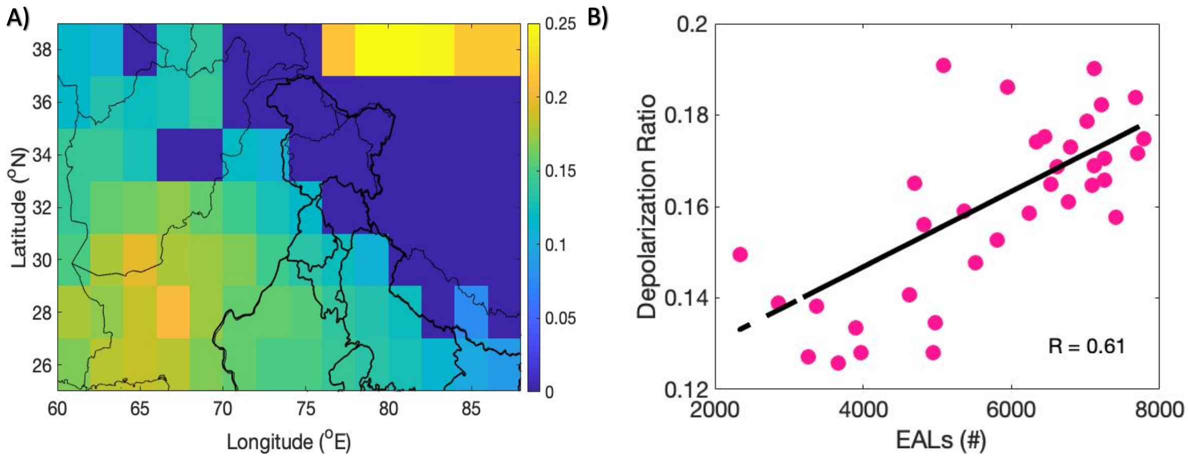

Supplementary Figure 1: Panel A shows the spatial distribution of climatological mean depolarization ratio for detected EALs on latitude-longitude map. Higher depolarization ratios indicate the dominance of non-spherical dust particles. EALs located within altitudes of 2 to 6 km are integrated and temporally averaged across MAMJJA of 2007-2016. Panel B illustrates the correlation between monthly mean depolarization ratio with the corresponding number of EALs detected during the 10 years (2007-2016; MAMJJA) from CALIPSO measurements over the Indus basin box shown in Figure 1D.

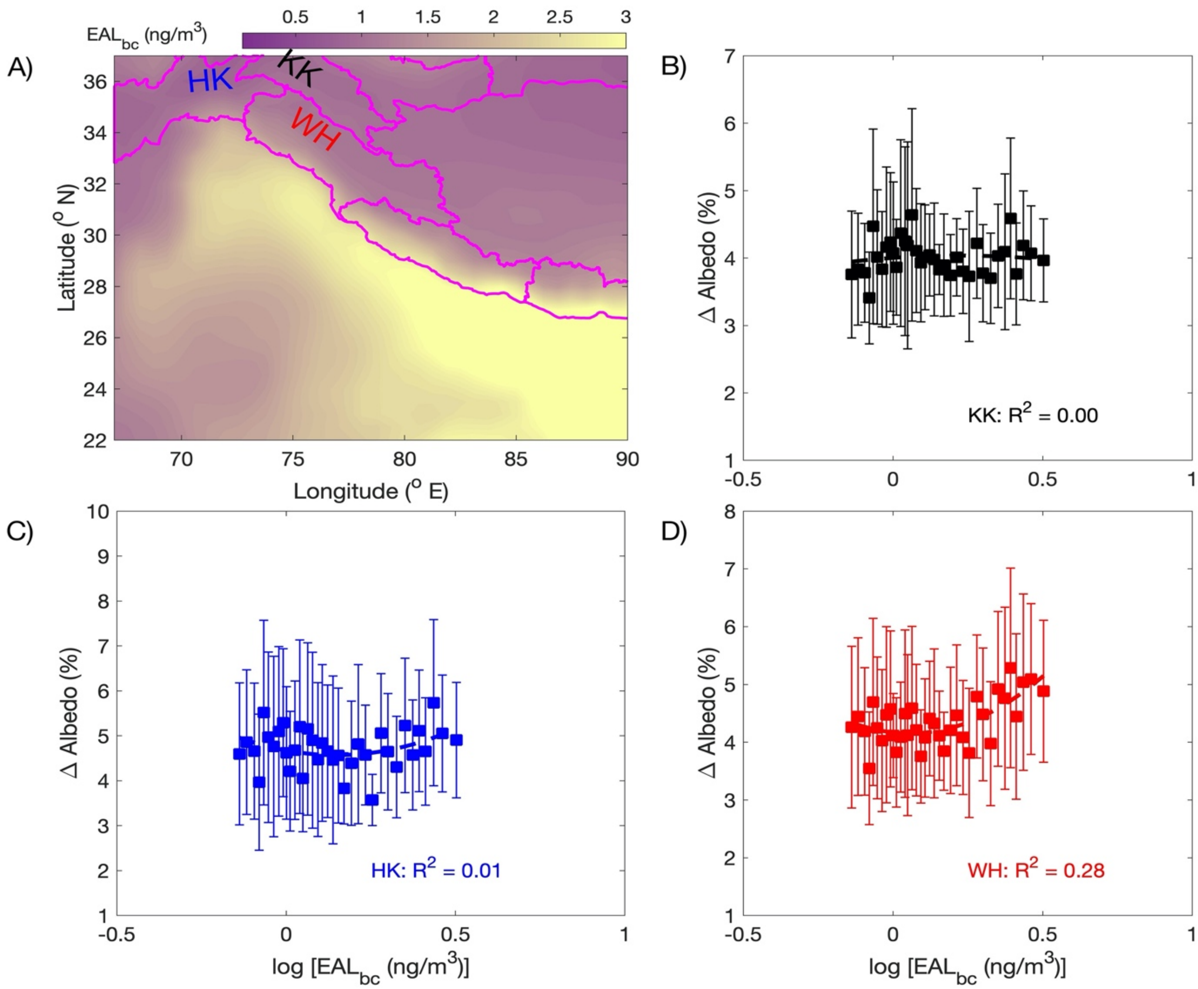

Supplementary Figure 2: Same as Figure 3, but for BC concentration in EALs from MERRA-2 reanalysis data.

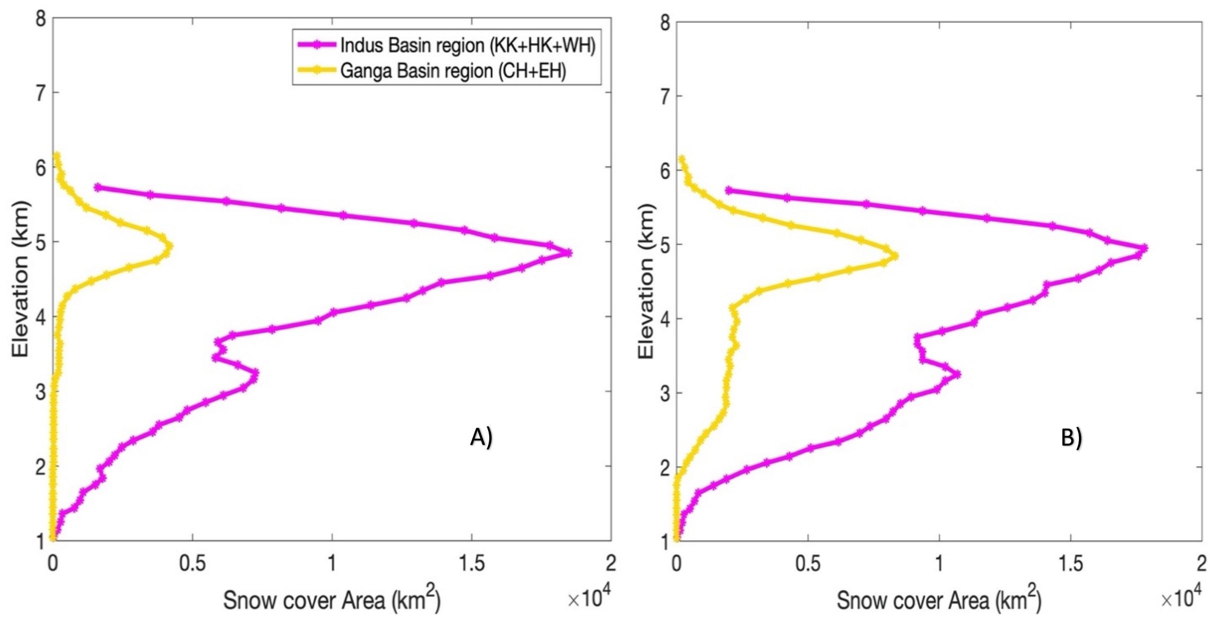

Supplementary Figure 3: Panels A and B compares the elevational variability in STC-MODSCAG estimated and WRF-Chem SNICAR simulated fractional snow cover area variation (annual mean snow fraction > 0.05), respectively.

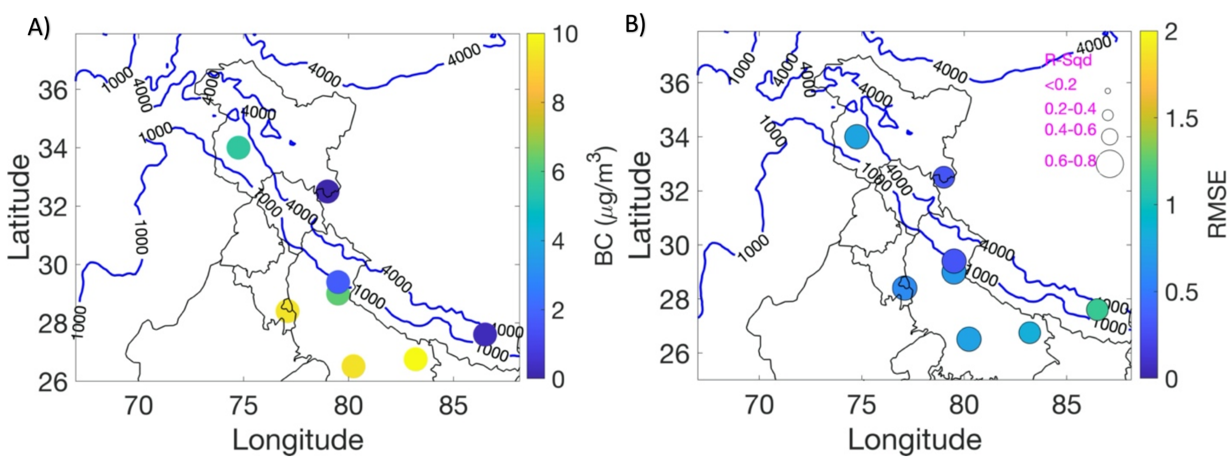

Supplementary Figure 4: Panel A illustrates the spatial distribution of measured annual mean BC concentration at surface at various sites as reported in Nair et al., 2013 and references therein. Panel B illustrates the correlation coefficient (the size of the marker) and the RMSE (the color) between modelled BC in surface layer and corresponding measured data at monthly resolution. The pink lines indicate surface terrain in hPa. Unfortunately, no such data for dust is available.

A)

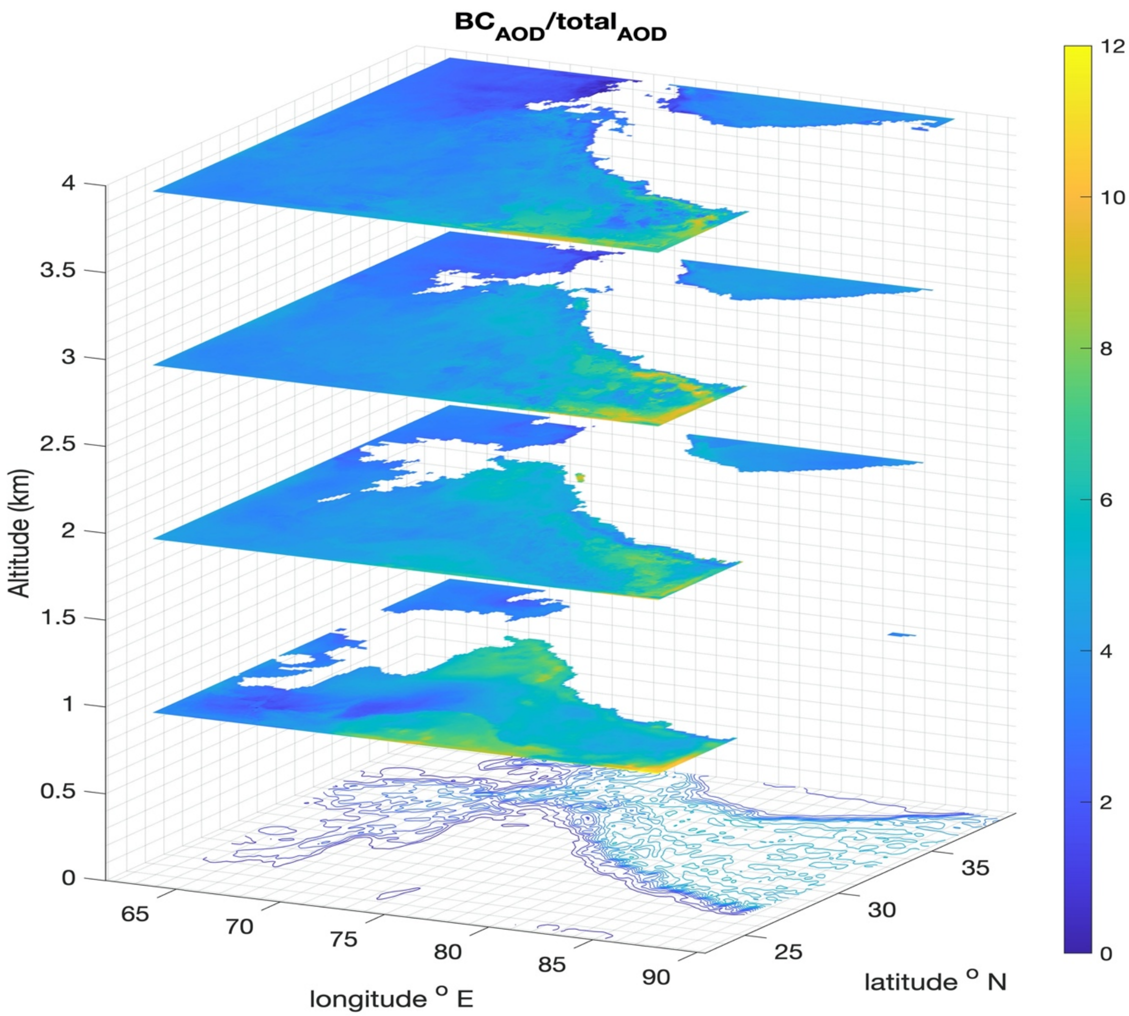

Supplementary Figure 5A: Panel shows the WRF-Chem-SNICAR simulated spatial distribution of contribution of BC-AOD to total AOD (in %) on Latitude-Longitude axes at 4 different altitude layers of ±0.5 km each. The bottom plane illustrates the terrain of HMA in contour lines.

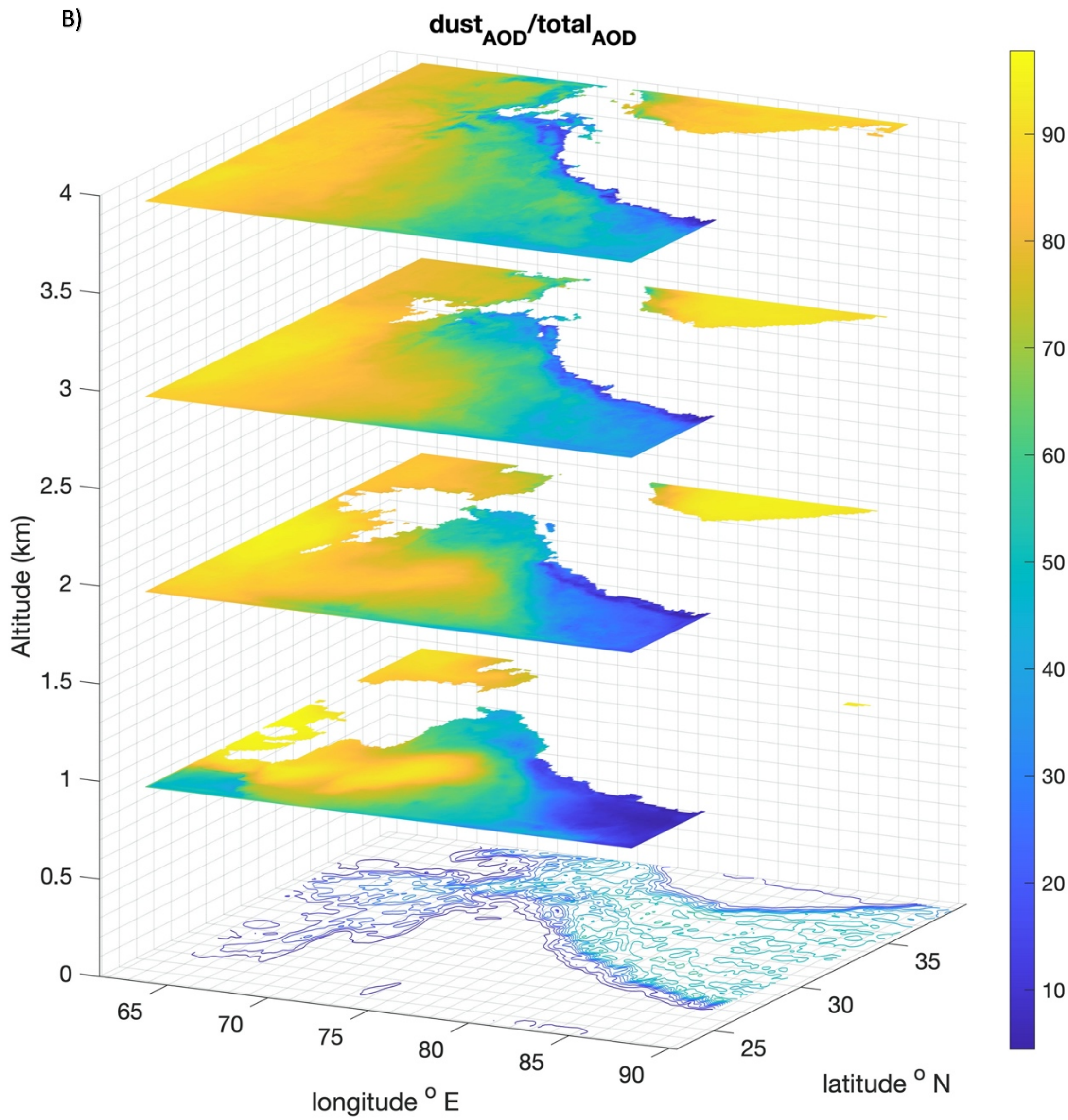

Supplementary Figure 5B: Same as Panel 5A, but for contribution of Dust-AOD to total AOD (in %). The bottom plane illustrates the terrain of HMA in contour lines.

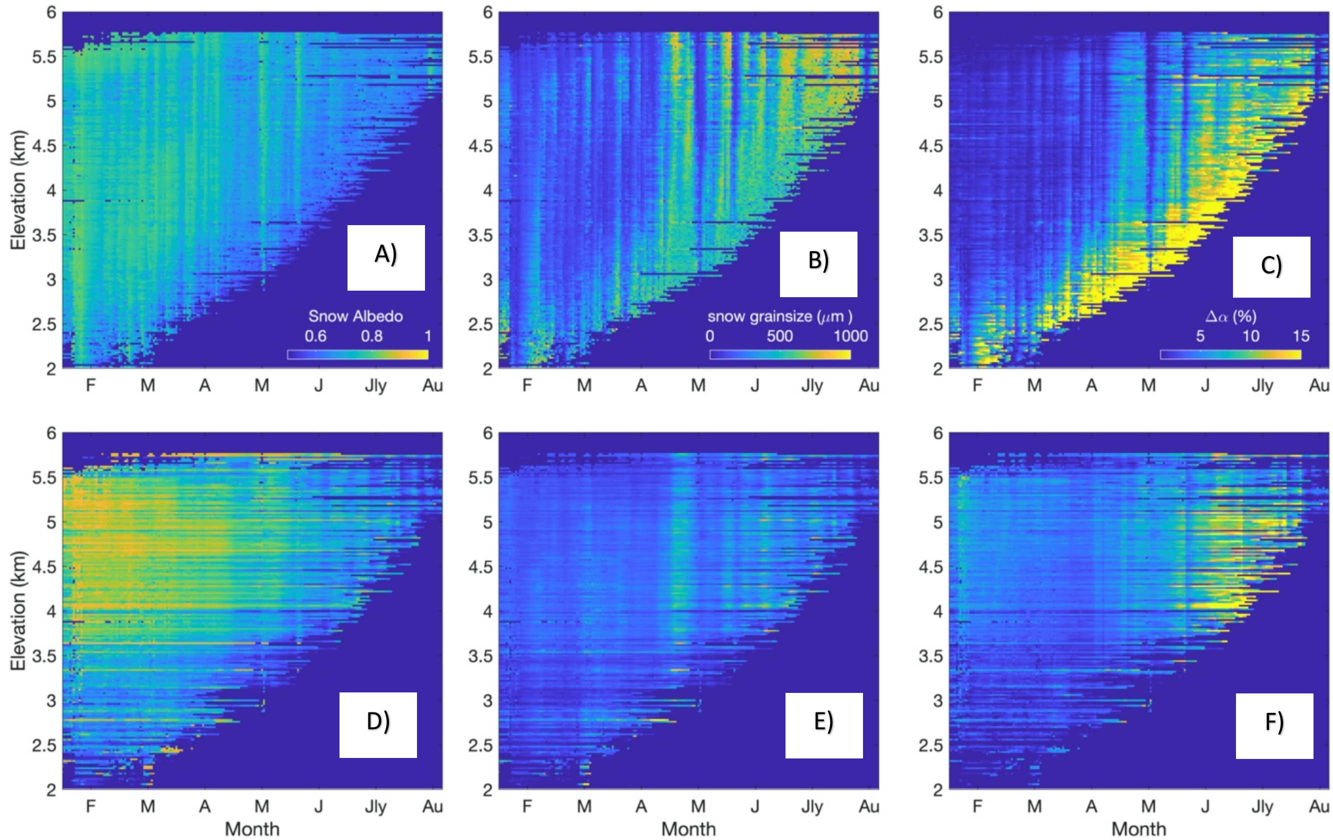

Supplementary Figure 6: Panels A-C illustrate the elevation-time evolution plots of WRF-Chem-SNICAR simulated daily midday mean snow surface albedo, Snow grain size and LAP-induced snow albedo reduction, respectively. The variables in grids present in Western Himalayas, Karakoram and Hindukush sub-regions (representative of western HMA) are segregated into elevational bins (of 20m each) and averaged. Panels D-E illustrates the corresponding values as estimated by STC-MODSCAG and STC-MODRFFS.

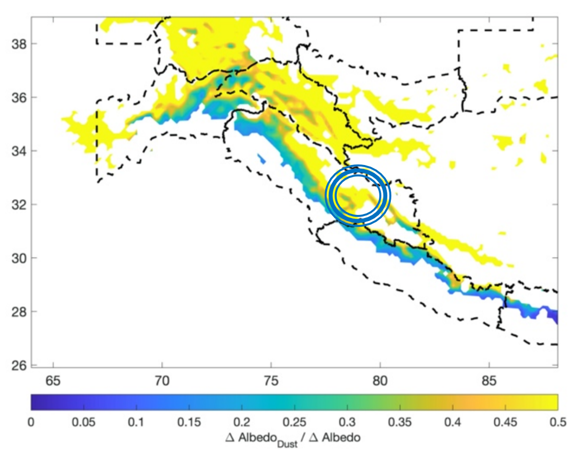

Supplementary Figure 7: WRF-Chem-SNICAR simulated ratio of dust-induced albedo reduction to total albedo reduction averaged over March-August.

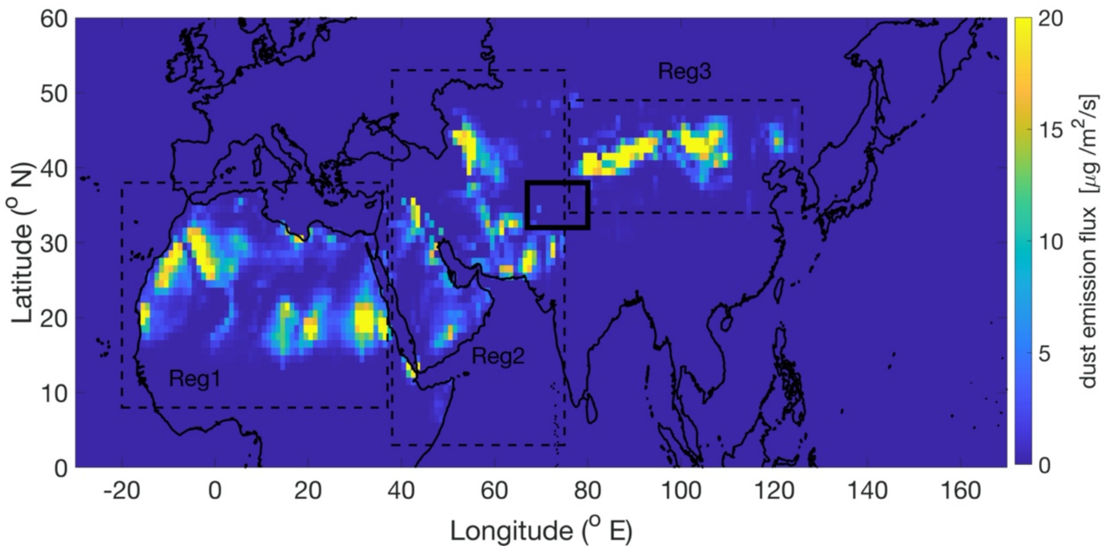

Supplementary Figure 8A: Spatial distribution of dust emission fluxes in a quasi-global WRF-Chem simulation around western HMA (black solid box). A tracer analysis is used to estimate the contribution of dust emissions from various regional sources to the dust deposition over western HMA. Dust tracers from three different dust emission regions (hashed black boxes) categorized by their distance from HMA are released in the model. The tracers are subjected to all the physical processes that determine the aerosol distribution. Reg 1 includes the Sahara Desert and other arid regions of Africa. Reg 2 includes the Thar Desert in India, Saudi Arabia and other arid regions of Afghanistan and Pakistan. Reg 3 includes the Gobi Desert and other arid regions of China and Mongolia.

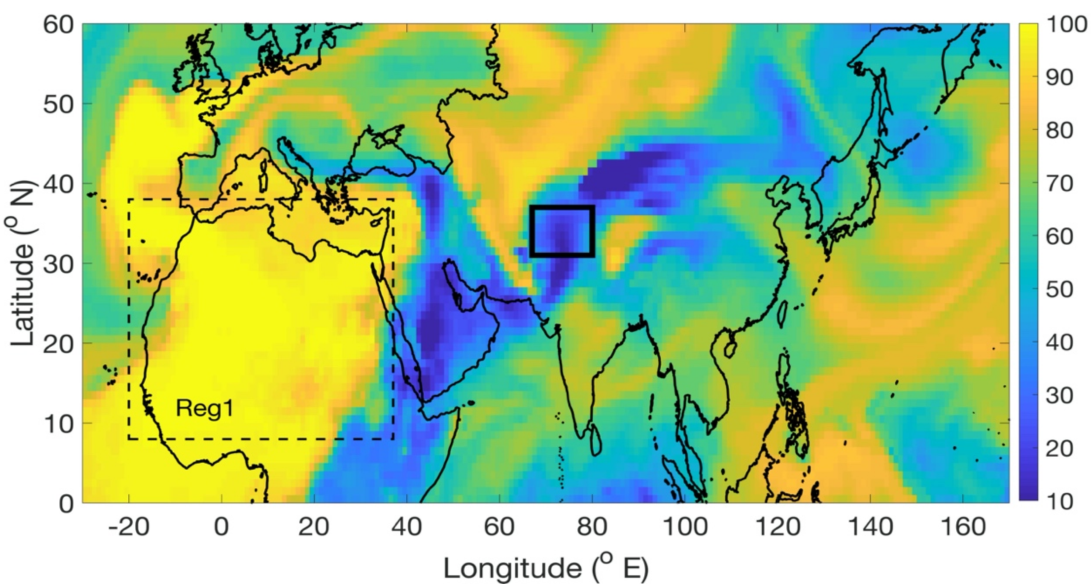

Supplementary Figure 8B Spatial distribution of the ratio of column integrated concentration of dust tracers from Reg 1 to the ambient dust burden at each grid. This ratio can be used as a first order estimate of the source contribution of Reg 1 dust emissions to dust over western HMA. The black solid box denotes western HMA. About 20% of the dust reaching western HMA is contributed from Reg 1 dust emissions.

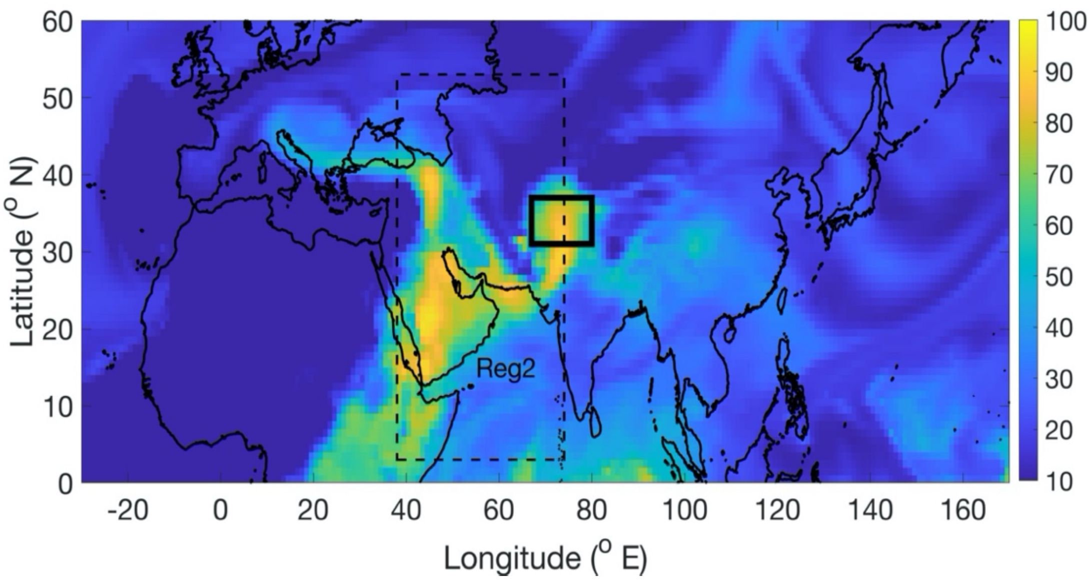

Supplementary Figure 8C Similar to Figure S8B, but for Reg 2 dust emissions. About 80% of the dust reaching western HMA is contributed from Reg 2 dust emissions, located upwind of HMA.

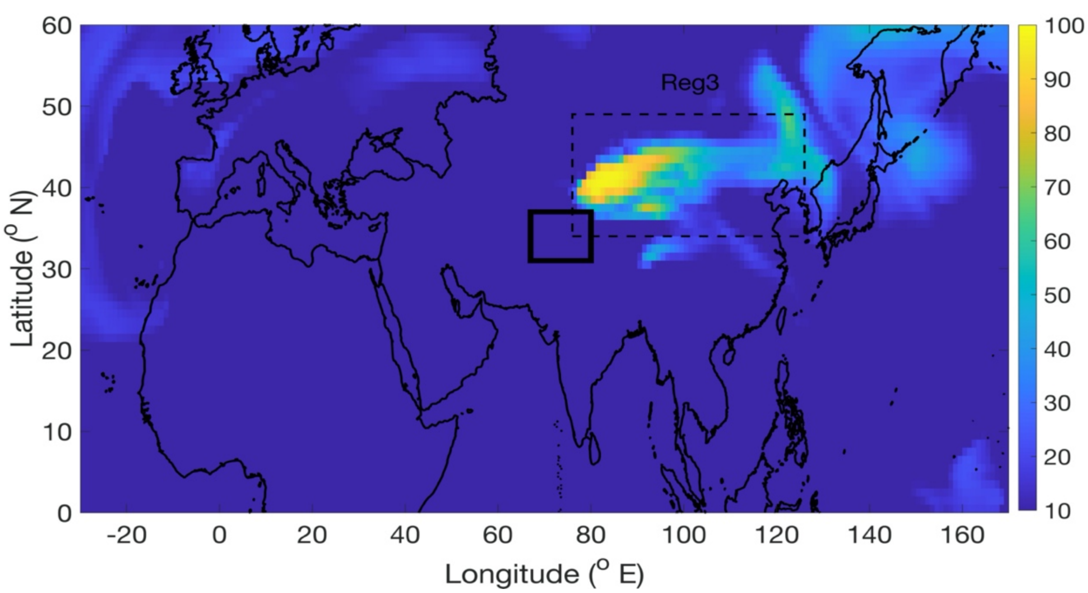

Supplementary Figure 8D Similar to Figure S8A, but for Reg 3 dust emissions. Reg 3 dust emissions have negligible contribution to the dust reaching western HMA as it is located downwind of the westerlies reaching HMA.

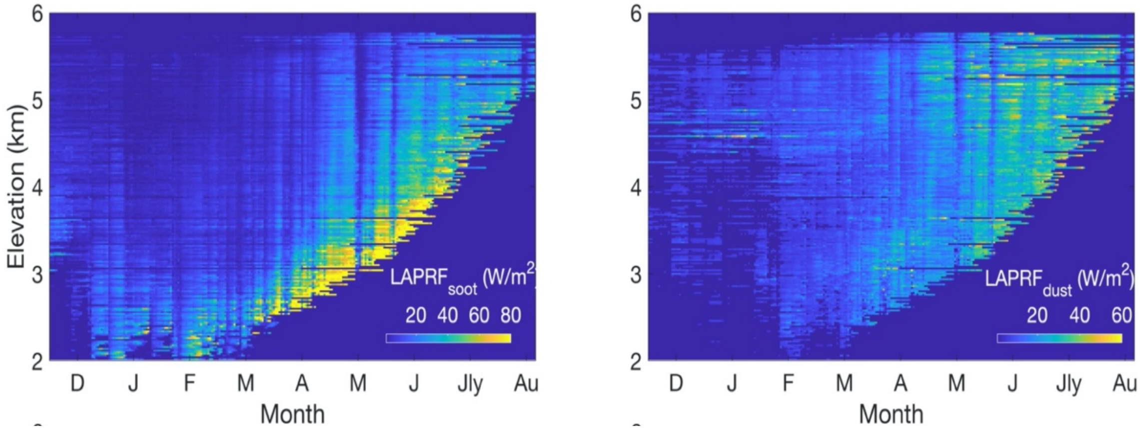

Supplementary Figure 9: Same as Supplementary Figure 6C, but for WRF-Chem-SNICAR simulated LAPRF$_{soot}$ (A) and LAPRF$_{dust}$ (B).

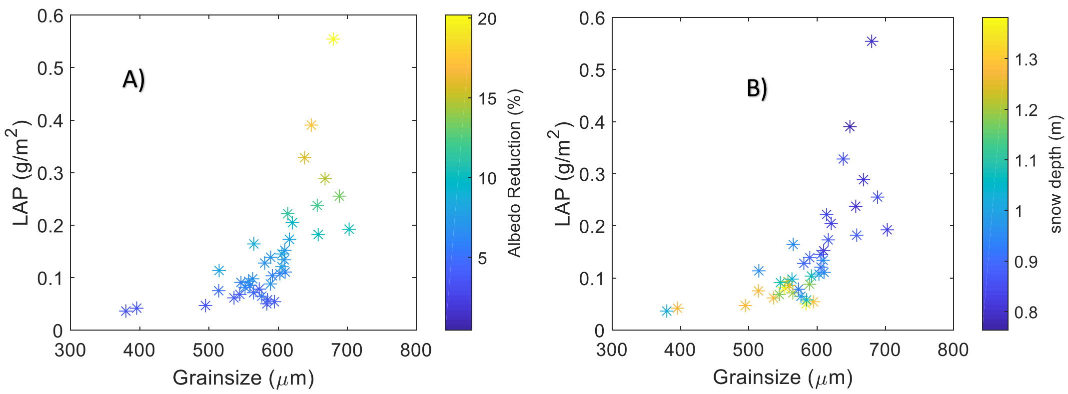

Supplementary Figure 10: WRF-Chem-SNICAR simulated coupling between A) LAP concentration-snow grain size and LAP-induced albedo reduction and B) LAP concentration-snow grain size and total snow depth during July and August month over a high elevation representative site in western Himalaya (bounded by blue circle in Supplementary Figure 7).

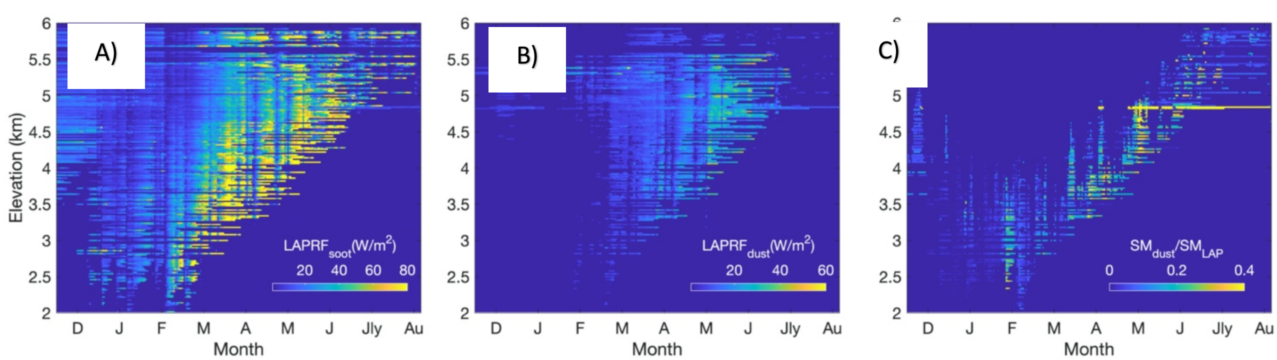

Supplementary Figure 11A and 11B: Same as Supplementary Figure 9A and B, but for central and eastern Himalaya mountain ranges i.e. Ganga basin region of HMA. Supplementary Figure 11C is same as Figure 5B, but for eastern HMA i.e. Ganga basin region of HMA.